

# Transport across nanogaps using semiclassically consistent boundary conditions

Debabrata Biswas, Pradeep Baraila, and Raghwendra Kumar

Theoretical Physics Division, Bhabha Atomic Research Centre, Mumbai 400 085, INDIA

(Dated: 6 September 2018)

Charge particle transport across nanogaps is studied theoretically within the Schrodinger-Poisson mean field framework and the existence of limiting current investigated. It is shown that the choice of a first order WKB wavefunction as the transmitted wave leads to self consistent boundary conditions and gives results that are significantly different in the non-classical regime from those obtained using a plane transmitted wave. At zero injection energies, the quantum limiting current density ( $J_c$ ) is found to obey the local scaling law  $J_c \sim V_g^\alpha / D^{5-2\alpha}$  with the gap separation  $D$  and voltage  $V_g$ . The exponent  $\alpha > 1.1$  with  $\alpha \rightarrow 3/2$  in the classical regime of small de Broglie wavelengths. These results are consistent with recent experiments using nanogaps most of which are found to be in a parameter regime where classical space charge limited scaling holds away from the emission dominated regime.

The current-voltage characteristics across nanogaps is a subject of much interest across a wide variety of fields. An important quantity is the maximum current that can be transmitted across the gap. In classical physics, the limit exists due to the mutual repulsion between the charged particles and the current is said to be space charge limited. In a mean field picture, the mutual repulsion gives rise to a potential barrier. As the current reaches the limiting value, the barrier height increases and the transmitted particles barely cross the barrier. Beyond this value, the barrier height oscillates, some electrons get reflected and steady state transport is no longer possible. The Child-Langmuir<sup>1,2</sup> law and its many generalizations<sup>3-5</sup> serve well to predict the maximum transmitted current in macro devices where the available phase space volume is large and quantum effects can be safely ignored.

In nanostructures however, the small physical size together with low applied voltages or injection energies pushes the average per electron phase space volume towards the plank cell limit. Thus, in addition to space charge, quantum effects must be considered in exploring the existence of such a limit in nanoelectronics, vacuum microelectronics or devices such as the scanning tunneling microscopes. In particular, the possibility of tunneling leads to the question: *is there a limit on the maximum transmitted current density in the quantum mechanical case?* Theoretical studies<sup>6,7</sup> suggest that quantum tunneling pushes up this limit and by orders of magnitude in the low injection energy regime where quantum effects should be considerably more important. In fact, within the framework considered in Ref. 6, the limit can indeed be very large in the *very low energy* regime as we shall show here. This singular behavior, signalling a sharp departure from the classical prediction, warrants a fresh look at the basic assumptions involved, especially since, many of them are retained in more sophisticated theories<sup>7-9</sup> which take into account the fermionic nature of electrons by incorporating the exchange-correlation potential.

In its simplest form, the mean field quantum (Hartree) formalism involves solving the coupled Schrodinger and Poisson equations

$$-\frac{\hbar^2}{2m} \frac{d^2\psi}{dx^2} - eV(x)\psi = E\psi \quad (1)$$

$$\frac{d^2V}{dx^2} = \frac{e|\psi|^2}{\epsilon_0} \quad (2)$$

in the region  $[0, D]$  where  $D$  is the size of the gap,  $e$  is the magnitude of the electronic charge,  $E$  is the energy of the electron and  $V(0) = 0$  while  $V(D) = V_g$ . Such a model is expected to hold when the electron density in the gap is sufficiently high that their mutual interaction must be accounted for, but is low enough to neglect the effects of the exclusion principle. It is assumed here that  $V$  is time-independent and there is a steady current flowing across the gap with a current density  $J = e\hbar(\psi^*\psi' - \psi\psi'^*)/2m$ . The boundary conditions or initial values for  $\psi$  are to be determined taking into account this fact.

Following Ref. 6, we write the wavefunction  $\psi$  as

$$\psi(x) = (n_s \bar{E})^{1/2} r(\bar{x}) e^{i\theta(\bar{x})} \quad (3)$$

where  $r(\bar{x})$  and  $\theta(\bar{x})$  are real,  $\bar{E} = E/eV_s$  is a dimensionless energy and  $n_s$  is a characteristic density. In terms of other dimensionless quantities  $\bar{x} = x/D$ ,  $\bar{V} = eV/E$ ,  $\bar{J} = J/J_s$ ,  $\bar{n} = n/n_s = |\psi|^2/n_s$  and  $\phi_g = eV_g/E$ , where  $V_s = \hbar^2/(2meD^2)$ ,  $J_s = \epsilon_0\hbar^3/(4m^2eD^5)$ ,  $n_s = \epsilon_0\hbar^2/(2me^2D^4)$ , the coupled Schrodinger and Poisson equations can be expressed as

$$\frac{d^2r}{d\bar{x}^2} + \bar{E}[(1 + \bar{V}) - \frac{(\lambda/4)^2}{r^4}]r = 0 \quad (4)$$

$$\frac{d^2\bar{V}}{d\bar{x}^2} = r^2 \quad (5)$$

$$\frac{d\theta}{d\bar{x}} = \frac{\lambda\bar{E}^{1/2}}{4r^2(\bar{x})} \quad (6)$$

where  $\lambda = 2\bar{J}/\bar{E}^{3/2}$  is a dimensionless perveance. Note that once  $r(\bar{x})$  is known,  $\theta(\bar{x})$  can be determined independently with an arbitrary phase ( $\theta(1) = 0$ ) at the boundary  $x = D$ .

Assuming now that at  $x \simeq D$ ,  $\psi(x) = Ce^{ip(D)x/\hbar}$ , it follows that  $r(1) = (\lambda/4)^{1/2}/(1 + \phi_g)^{1/4}$  while  $r'(1) = 0$ . Here  $p(x) = \sqrt{2m(E + eV(x))}$  is the classical momentum. Note that the plane wave assumption above presupposes a constant potential immediately beyond the domain of interest<sup>6</sup> irrespective of the nature of the interface at  $x = D$ , the length scales involved and the self consistent nature of the problem.

At a given scaled injection energy  $\bar{E}$ , the dimensionless perveance  $\lambda$  is increased till no solution exists. This gives the critical current density  $J_c = J_s \lambda_c \bar{E}^{3/2}/2$ . In Ref. 6, it has been observed that for small values of  $\bar{E}$ ,  $\lambda_c$  exceeds the classical values by orders of magnitude.

The behaviour of the system at low injection energies ( $\bar{E}$ ) can be analysed by neglecting the second term altogether in Eq. (4) at finite values of  $\lambda$ . It is then easy to see that at very low energies, a solution exists as  $\lambda$  is increased at least so long as the second term in Eq. (4) can be neglected. This behaviour is however peculiar to the initial conditions specified above. We show later that the same equations albeit with a different initial condition for  $r'(1)$  imposes a limit on  $\lambda$  beyond which no solution exists even at low injection energies.

Apart from the  $\bar{E} \rightarrow 0$  behaviour, the semiclassical consistency of the transmitted plane wave assumption is also worth investigating. If the potential  $\bar{V}$  for a particular value of  $\bar{E}$  and  $\lambda$  is well behaved in the region  $[0, D]$ , it is reasonable to expect that away from classical turning points of the potential  $\bar{V}$ , the transmitted wavefunction should have the standard first order WKB form:

$$\psi_{sc}(x) = \frac{C}{\sqrt{p(x)}} e^{\frac{i}{\hbar} \int^x p(x') dx' + i\varphi} \quad (7)$$

as  $x$  approaches  $D$ . Here  $p(x)$  is the classical momentum while  $C$  is assumed to be real with all the phase information dumped in  $\varphi$ . Assuming this form to be true at  $x = x_0 < D$ , it is possible to compare  $r(\bar{x})$  and  $\theta(\bar{x})$  with the semiclassical amplitude and phase by integrating backwards from  $\bar{x}_0 = x_0/D$ . Thus, starting with  $r(\bar{x}_0) = r_{sc}(\bar{x}_0) = C/\sqrt{p(\bar{x}_0)}$  and  $\theta(\bar{x}_0) = \theta_{sc}(\bar{x}_0) = \int^{x_0} p(x') dx'/\hbar + \varphi$ , one can compare  $r(\bar{x})$  and  $\theta(\bar{x})$  for values of  $x < x_0$  with the semiclassical (WKB) predictions:  $r_{sc}(\bar{x}) = C/\sqrt{p(\bar{x})}$  and  $\theta_{sc}(\bar{x}) = \int^x p(x') dx'/\hbar + \varphi = \theta(\bar{x}_0) - \int_x^{x_0} p(x') dx'/\hbar$ . A comparison of the amplitudes for  $\bar{E} = 1$  and 1000 is shown in Fig. 1 for  $\lambda = 15$  and  $\phi_g = 0.5$ . While  $\theta(\bar{x})$  and  $\theta_{sc}(\bar{x})$  agree reasonably at  $\bar{E} = 1$  near  $\bar{x}_0 = 0.9$  (not shown here), the amplitude  $r(\bar{x})$  has very little agreement with  $r_{sc}(\bar{x})$  even slightly away from  $\bar{x} = \bar{x}_0$  (see Fig. 1). At  $\bar{E} = 1000$  however, the amplitude oscillates about the semiclassical prediction while  $\theta(\bar{x})$  and  $\theta_{sc}(\bar{x})$  are practically indistinguishable in the entire region.

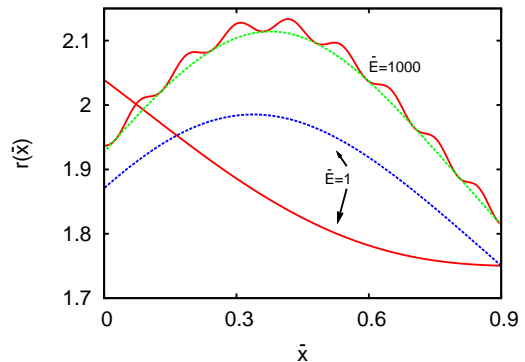


FIG. 1. (Color online) A comparison of the amplitude  $r(\bar{x})$  obtained using the plane wave boundary condition with the semiclassical prediction  $r_{sc}(\bar{x})$  (dashed curves). The agreement is poor at  $\bar{E} = 1$  but improves for  $\bar{E} = 1000$ . Here  $\lambda = 15$  and  $\phi_g = 0.5$  while  $\bar{x}_0 = 0.9$ .

These results are indeed not very surprising since the plane wave approximation is only the first term in a semiclassical expansion of  $\psi(x) = e^{\frac{i}{\hbar} S(x)}$ :  $S(x) = S_0(x) + \frac{\hbar}{i} S_1(x) + (\frac{\hbar}{i})^2 S_2(x) + \dots$  where  $S_0(x) = \int^x p(x') dx'$ . By dropping  $S_1$  and subsequent terms in a plane wave expansion, it is only to be expected that the amplitude is not reproduced accurately even for large  $\bar{E}$  while the phase information is well approximated as  $\bar{E}$  increases.

For a well behaved potential, a better approximation for the transmitted wave near  $x = D$  should be the first order WKB wavefunction in Eq. (7), while for  $x \simeq 0$ , it should be a superposition of a right and a left moving wave of the WKB form:  $\psi_{sc}(x \simeq 0) = (A/\sqrt{p(x)})e^{\frac{i}{\hbar} \int^x p(x') dx'} + (B/\sqrt{p(x)})e^{-\frac{i}{\hbar} \int^x p(x') dx'}$ .

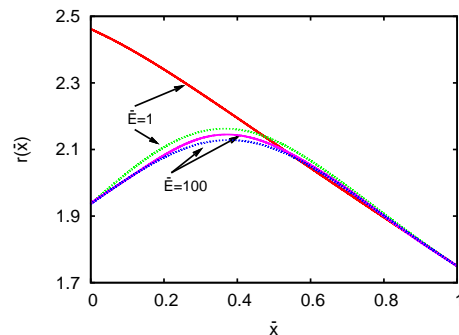


FIG. 2. (Color online) A comparison of the amplitude  $r(\bar{x})$  obtained using the new initial condition with the WKB prediction  $r_{sc}(\bar{x})$  for  $\lambda = 15$  and  $\phi_g = 0.5$ . The agreement is better even at  $\bar{E} = 1$ . At  $\bar{E} = 100$ , there is practically no reflection. The agreement is therefore good even near  $\bar{x} = 0$ . The solid lines are the exact results; the dashed/dotted lines are the WKB predictions.

Assuming the semiclassical form (Eq. (7)) to be valid at  $x = D$ , the initial conditions for  $r(\bar{x})$  are  $r(1) =$

$(\lambda/4)^{1/2}/(1+\phi_g)^{1/4}$  and  $r'(1) = -\bar{V}'(1)\lambda^{1/2}/[8(1+\phi_g)^{5/4}]$ . Note that  $r'(1)$  depends on  $\bar{V}'(1)$ . This does not preclude  $r'(1) = 0$ ; rather it forces the potential to assume a constant value smoothly at  $x \simeq D$  in order to be semiclassically consistent<sup>10,11</sup>. In practice, Eqns. (4) and (5) are solved as an initial value problem starting at  $\bar{x} = 1$  and integrating backwards till  $\bar{x} = 0$  by choosing a value for  $\bar{V}'(1)$  such that  $\bar{V}(0) = 0$ <sup>12</sup>. For the parameter values studied by us however,  $\bar{V}'(1) \neq 0$  for any allowed solution set. Not surprisingly, a comparison of  $r(\bar{x})$  and  $r_{sc}(\bar{x})$  shows a much better agreement now as shown in Fig. 2.

Imposition of the semiclassical boundary condition also removes the singular behaviour at low scaled energies ( $\bar{E} \rightarrow 0$ ). Neglecting the second term in Eq. (4), and using the new initial conditions, the amplitude equation gives  $r(\bar{x}) = a\bar{x} + b$  where  $a + b = (\lambda/4)^{1/2}/(1+\phi_g)^{1/4}$  and  $a = -\bar{V}'(1)\lambda^{1/2}/[8(1+\phi_g)^{5/4}]$ . Inserting  $r(\bar{x})$  in the Poisson equation (Eq. 5) and using the boundary condition  $\bar{V}(0) = 0$  gives  $\bar{V}(\bar{x}) = a^2\bar{x}^4/12 + ab\bar{x}^3/3 + b^2\bar{x}^2/2 + c\bar{x}$ . Finally on using  $\bar{V}(1) = \phi_g$  and demanding that  $r'(1) = -(a^3/3 + ab + b^2 + c)\lambda^{1/2}/[8(1+\phi_g)^{5/4}]$ , a real solution is found to exist only when  $(48\mathcal{E}^6)^2 - (96\mathcal{E}^6 + 12\mathcal{E}^2\phi_g)\lambda - \lambda^2/2 > 0$  where  $\mathcal{E} = (1+\phi_g)^{1/4}$ . This imposes an upper limit on the perveance  $\lambda$  at low injection energies which matches with the critical perveance  $\lambda_c$  at small  $\bar{E}$  obtained by solving the full set of equations (Eqns. (4) and (5)) for different values of  $\lambda$ . For instance, the inequality above predicts that a real solution exists at  $\phi_g = 0.5$  for  $\lambda < 38.33$  at very small values of  $\bar{E}$ . This is a good approximation to the actual value at small  $\bar{E}$  as can be seen in Fig. 3 where  $\lambda_c$  is plotted for different scaled injection energies for  $\phi_g = 0.5, 0$  and  $-0.5$ . Note that  $\lambda_c$  does not increase by orders of magnitude even at low injection energies. Rather the quantum regime manifests itself differently at various applied potentials. While  $\lambda_c$  is about double the classical value at  $\phi_g = 0.5$ , it is less than the classical value at  $\phi_g = -0.5$  where reflection (rather than tunneling) dominates. In general, at most injection energies, the maximum current evaluated quantum mechanically falls short of the classical prediction.

When the injection energy is exactly zero, ( $E = 0$  in Eq. (1)), the semiclassical formalism in the space charge limited regime is similar but the equations and initial conditions are slightly different<sup>13</sup>. It is interesting to investigate whether the scaling relationship with applied voltage is different from the classical  $V_g^{3/2}$  law of Child-Langmuir with the new boundary condition. The variation of the scaled critical current  $\bar{J}_c = J_c/J_s$  with  $\bar{U}_g = V_g/V_s$  is shown in Fig. 4. Clearly,  $\bar{J}_c \sim \bar{U}_g^\alpha$  locally with the exponent in the range  $1.1 \leq \alpha \leq 1.5$  and converging to 1.5 as  $\bar{U}_g$  is increased. Note that  $\bar{U}_g = V_g/V_s \sim V_g D^2$  while  $\bar{J}_c = J_c/J_s \sim J_c D^5$ . Thus  $J_c D^5 \sim V_g^\alpha D^{2\alpha}$  or

$$J_c \sim \frac{V_g^\alpha}{D^{5-2\alpha}} \quad (8)$$

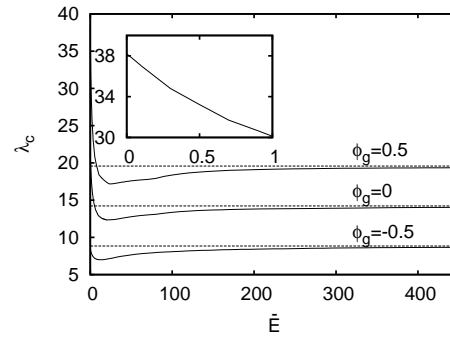


FIG. 3. The critical perveance  $\lambda_c$  is plotted against  $\bar{E}$ . The dashed lines are the classical prediction while the solid lines are obtained by numerically solving Eqns. (4) and (5). Inset shows the value of  $\lambda_c$  at small  $\bar{E}$  for  $\phi_g = 0.5$ .

Thus, as  $V_g$  and  $D$  are increased,  $J_c$  obeys classical scaling. Note that the  $\alpha = 1/2$  behaviour reported in Ref. 7 is not seen in our computations with the first order WKB boundary conditions. It is in fact possible to show<sup>13</sup> that the plane wave boundary condition predicts  $\alpha = 1/2$ . To see this, note that  $\bar{J} \sim \bar{U}_g^{1/2} \bar{n}(1)$  where  $\bar{n}(1) = q^2(1)$  and  $\psi(x) = q(\bar{x})\sqrt{n_s}e^{i\theta(\bar{x})}$ . Since

$$\frac{d\bar{n}}{d\bar{U}}|_{\bar{U}=\bar{U}_g} = \frac{d\bar{n}}{d\bar{x}}|_{\bar{x}=1} \frac{d\bar{x}}{d\bar{U}}|_{\bar{U}=\bar{U}_g} \quad (9)$$

and  $q'(1) = 0$  for a plane wave boundary condition,  $d\bar{n}/d\bar{U}|_{\bar{U}=\bar{U}_g} = 0$ . Thus,  $\bar{n}(1)$  is independent of  $\bar{U}_g$ . It follows that  $J \sim V_g^{1/2}/D^4$  only if the transmitted wavefunction is assumed to be a plane wave.

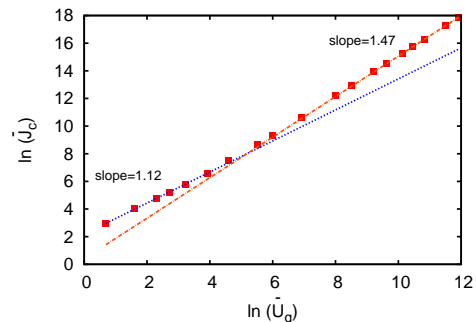


FIG. 4. (Color online) The scaled critical current  $\bar{J}_c$  follows a local power law relationship with the scaled applied voltage:  $\bar{J}_c \sim \bar{U}_g^\alpha$ . Boxes mark the numerically obtained values while the short and long dashed lines are the fits at small and large  $\bar{U}_g$  respectively. At small  $\bar{U}_g$ ,  $\alpha \simeq 1.12$  while for large  $\bar{U}_g$ ,  $\alpha \rightarrow 1.5$ .

Note that the smallest value<sup>14</sup> of the scaled potential considered is  $\bar{U}_g = 2$ . At  $D = 10\text{nm}$ , this translates to an applied potential of  $0.75\text{mV}$  while at  $D = 70\text{nm}$ ,

it is 0.015mV. On the higher side where classical scaling holds, the maximum scaled potential considered is  $\bar{U}_g = 150000$ . At  $D = 10\text{nm}$ , the maximum  $V_g = 57\text{V}$ , while at  $D = 70\text{nm}$ , the maximum applied voltage considered is  $V_g = 1.16\text{V}$ . Beyond these voltages, classical scaling should be applicable. These results are consistent with recent experiments on aluminium<sup>15</sup> and graphene<sup>16</sup> nanogaps. In case of aluminium for instance (see fig. 3 of Ref. 15), the 70nm gap shows good agreement with the Fowler-Nordheim emission law for  $V_g \lesssim 6\text{V}$ . Above this (see Fig. 4 of Ref. 15), the current appears to be space charge limited with the exponent  $\alpha \simeq 1.5$  which is consistent with the first order WKB results presented here.

In case of graphene<sup>16</sup>, the space charge limited regime occurs at smaller voltages possibly on account of Klein tunneling<sup>17</sup>. For a few hundred nanometer gap, the exponent  $\alpha$  averaged over several gate voltages, takes the classical space charge limited value of 1.5 for  $V_g \gtrsim 3\text{V}$ . This is again consistent with the results presented here.

In conclusion, we have shown that a first order WKB approximation for the transmitted wave gives semiclassical consistent results which are significantly different from those obtained using a plane transmitted wave. The maximum transmitted current is found to be smaller than the classical current for most injection energies and may exceed only in the quantum limit of small  $E$ . Finally, at zero injection energy, the limiting current density follows

a local scaling law  $J_c \sim V_g^\alpha/D^{5-2\alpha}$  with  $\alpha \rightarrow 3/2$  for large  $V_g$  and  $D$ . Importantly, our result using first order WKB approximation<sup>14</sup> underscores the possible parameter regime where nonclassical space charge limited behaviour may be observed experimentally.

<sup>1</sup>C. D. Child, Phys. Rev. Ser. 1 **32**, 492 (1911).

<sup>2</sup>I. Langmuir, Phys. Rev. **2**, 450 (1913).

<sup>3</sup>Y. Y. Lau, Phys. Rev. Lett. **87**, 278301 (2001).

<sup>4</sup>J. W. Luginsland, Y. Y. Lau and R. M. Gilgenbach, Phys. Rev. Lett. **77**, 4668 (1996).

<sup>5</sup>R. R. Puri, D. Biswas and R. Kumar, Phys. Plasmas **11**, 1178 (2004).

<sup>6</sup>Y.Y.Lau, D.Chernin, D.G.Colombant and P.-T.Ho, Phys. Rev. Lett. **66**, 1446 (1991).

<sup>7</sup>L. K. Ang, T. J. T. Kwan, and Y. Y. Lau, Phys. Rev. Lett. **91**, 208303 (2003).

<sup>8</sup>W. S. Koh and L. K. Ang, Nanotechnology, **19**, 235402 (2008).

<sup>9</sup>L. K. Ang, W. S. Koh, Y. Y. Lau and T. J. T. Kwan, Phys. Plasmas **13**, 056701 (2006).

<sup>10</sup>Semiclassical boundary conditions have been used before; see<sup>11</sup>

<sup>11</sup>S. J. Singer, S. Lee and K. F. Freed, J. Chem. Phys., **91**, 240 (1989).

<sup>12</sup>There are two sets of solutions which merge as the critical current is approached. We choose the one with the lower potential energy.

<sup>13</sup>The details will be presented in a separate communication.

<sup>14</sup>At very small spacings or applied voltages, higher order WKB wavefunctions may be required.

<sup>15</sup>S. Bhattacharjee and T. Chowdhury, App. Phys. Lett. **95**, 061501 (2009).

<sup>16</sup>H. M. Wang, Z. Zheng, Y. Y. Wang, J. J. Qiu, Z .B. Guo, Z. X. Shen, and T. Yu, App. Phys. Lett. **96**, 023106 (2010).

<sup>17</sup>S. Sun, L. K. Ang, D. Shiffler and J. W. Luginsland, App. Phys. Lett. **99**, 013112 (2011).